Coordination and competition between magnetic particles driven by opposite climate transitions

Yunfeng Cai[1], Xiaoyong Long[1*], Xianqiang Meng[2], Junfeng Ji[3], Yong Wang[1], Shiyou Xie[1]

[1]School of Geographical Sciences, Southwest University, Chongqing, China

[2] State Key Laboratory of Lake Science and Environment, Nanjing Institute of Geography and Limnology, Chinese Academy of Sciences, Nanjing, China

[3]Institute of Surficial Geochemistry, College of Earth Sciences and Engineering, Nanjing University, Nanjing, China

*Corresponding author: Xiaoyong Long (longxy@126.com)

Key Points:

- Dry and warm climates favor the dehydration of amorphous iron oxides to form antiferromagnetic hematite and ferrimagnetic particles
- Wet and cool climates retard their formation but lead to competition
- Evaporation is as important as precipitation in extreme climate cycles and patterns reconstruction

Abstract

The ferrimagnetic (FM) and antiferromagnetic (AFM) particles of iron oxides are considered to be pedogenic and climatic indicators in soil taxonomy and paleoclimate reconstruction due to their enrichment trends as a function of increasing rainfall and temperature. However, opposite climate can retard chemical weathering but promote significant transformation between iron oxides, which could account for a nonlinear response of magnetism and color to extreme climate. We examined two soil sequences undergone opposite climate on the eastern edge of the Tibetan Plateau. The dry and warm climate transition favors the dehydration of amorphous iron oxides to form AFM hematite and FM particles, while the wet and cool climate transition impedes the formation but leads to their competition. The outcome well interprets the synchronous and asynchronous changes in color and magnetism under extreme opposite climate, and suggests that evaporation is as important as precipitation in extreme paleoclimate reconstructions based on iron oxides.

Key words: Magnetism; Color; Iron oxides; Paleoclimate reconstruction

Plain Language Summary

Iron oxides are ubiquitous on the surface of Earth and Mars. They can be divided into antiferromagnetic (AFM) and ferrimagnetic (FM) phases according to physical properties. The former is found in colors ranging from red to yellow, while the latter is the dominant form of magnetism in soils and sediments. Color and magnetism are considered sensitive pedogenic and climatic indicators in soil taxonomy and paleoclimate reconstruction because iron oxides are commonly enriched as a result of increasing regional rainfall and temperature. However, inverse changes in temperature with rainfall can retard chemical weathering but promote significant transformation between FM and AFM particles, which could result in a nonlinear climatic response of soil color and magnetism to extreme climate cycles and patterns. The uplift of the Tibetan Plateau (TP) has led to different orographic lifts in the Yunnan Plateau (YP) and Guizhou Plateau (GP) on the eastern edge, which has resulted in contrasting climate transitions on both plateaus. We found that the dry and warm climate transition present in the YP is favorable to the dehydration of amorphous iron oxides that then synchronously form FM particles and AFM hematite, while the wet and cool climate transition present in the GP retards the formation but leads to their competition. It well interprets synchronous and asynchronous change of magnetism and color in dry and wet climate stages. Additionally, it also suggested that evaporation is as important as precipitation when performing extreme paleoclimate reconstruction based on iron oxides, especially during extreme climate cycles and patterns.

1 Introduction

Iron oxides are ubiquitous on the surface of Earth and Mars [*Cornell and Schwtermann, 2003; Christensen et al., 2001*] and can be divided into chromogenic and magnetogenic groups according to their physical properties [*Long et al., 2011*]. The former includes antiferromagnetic (AFM) hematite (Hm, α-Fe_2O_3) and goethite (Gt, α-FeOOH) dominate optical properties, while the latter includes ferrimagnetic

(FM) magnetite (Mgt, Fe_3O_4) and maghemite (Mgh, γ-Fe_2O_3), which dominate magnetism in soils and sediments [*Cornell and Schwartzman, 2003; Liu et al., 2012*]. These particles are often synchronously enriched as immobile weathering products under aerobic conditions with comparable increase in rainfall and temperature [*Long et al., 2011, 2016; Torrent et al., 2006*]. Consequently, color and magnetism are considered reasonable pedogenic and climatic indicators in soil taxonomy and paleoclimate reconstruction if iron contents in parent materials are comparable [*Cornell and Schwartzman, 2003; Maher,1998*]. Over the past few decades, magnetic properties have been successfully incorporated into paleorainfall reconstruction, especially with aeolian sediments in the Chinese Loess Plateau (CLP) [*Heller et al, 1991, 2010; Liu et al., 1995, 2003; Liu et al., 2007; Nie et al., 2008, 2013; Maher, 2016*] and other temperate regions [*Liu et al., 2001,2012; Chlachula, 2003*]. Meanwhile, the color indices of soils have also been employed to reflect changes in temperature [*Yang et al., 2001; Yang and Ding, 2003*].

However, growing evidences have been accumulated on asynchronous of color indices and magnetism properties in soils [*Han et al., 1996; Gao et al., 2018; Maher, 1998; Yang et al., 2001*] and sediments at different scales, especially in loesses and paleosols layers of CLP, such as S1 [*Liu and Ding, 1998*], S5 [*Guo et al., 2013*], and S9 [*Xie et al., 2003*], driven by extreme climate cycles, or deposits ranging from the Tertiary red clay to the Quaternary loess driven by the dramatic climate pattern shifts of the CLP [*Ji et al., 2004; Nie et al., 2014; Balsam et al., 2004; Hao et al., 2009*]. Therefore, the other soil chemical and mineral parameters have been introduced to understand these shifting correlations. The Fe_d parameter indicating the total amount of iron oxides has been applied to trace the changes in pedogenic intensity [*Ding et al., 2001*]. The Fe_o parameter reflecting amorphous iron oxides was also introduced to interpret the formation and transformation of FM particles [*Hu et al., 2009*]. Moreover, the ratio of Hm and Gt determined by diffuse reflectance spectra method [*Ji et al., 2001*] is used to reconstruct changes in the relative humidity (RH) rather than individual changes in rainfall and temperature [*Ji et al., 2001, 2004; Balsam, 2004; Hao et al., 2009*]. It was found that these extreme stages are often characterized by high pedogenic intensity [*Ding et al., 2002*], lower iron oxide crystallinity [*Hu et al., 2009*] and significant changes in Hm/(Hm+Gt) [*Ji et al., 2004; Hao et al., 2009*].

Theoretically, AFM Hm forms under warm, dry and seasonal climates, while Gt forms under cool, wet and less seasonal climates [*Schwertmann, 1985*]. The change in Hm/(Hm+Gt) can be promoted by inverse changes in rainfall and temperature [*Long et al., 2011, 2016*]. Moreover, FM Mgh particles with differing sizes compete with AFM Hm as an intermediate product from amorphous iron oxides under aerobic conditions [*Barrón and Torrent, 2002; Torrent, 2015*], which also depends on the formation efficiency of the Hm estimated by Hm/(Hm+Gt) [*Hu et al., 2013; Long et al., 2015*]. However, the pedogenesis derived from aeolian sediments is disturbed by the dust provenances [*Li et al., 2009*], deposition rates [*Kukla, 1987*], physical erosion processes [*Lu et al., 2006*] besides chemical weathering controlled by specific climates. Therefore, it is difficult to discern the independent contributions of climate to pedogenic iron oxides and related changes in color and magnetism.

The Yunnan Plateau (YP) and Guizhou Plateau (GP) on the eastern edge of the Tibetan Plateau (TP) have undergone differential uplifts and opposite climate transitions at least since the Quaternary [*Yang et al., 2010; Yan et al., 2011*] due to the uplift of the TP [*Pan et al., 2004*]. Moreover, the change in rainfall is accompanied by the inverse pattern of temperature, which enhance the difference in the relative humidity (RH) of the two plateaus. As a result, marked soil reddening in the YP and yellowing in the GP has been observed and indicates that the iron oxide transformations are driven by opposite climate transitions. These conditions provide a good opportunity to understand the correlation between chromogenic and magnetogenic iron oxides and their climatic implications in extreme wet-dry cycles and patterns.

2 Materials and Methods

2.1 Geographical settings and soil sampling

The YP and GP belong to the tectonic extrusion zone of the TP [*Bao et al., 2015*]. Compared to the flatter TP with that has experienced rapid uplifting to an average altitude of approximately 4000 m [*Li and Fang, 1999*], the surfaces of the YP and GP are rugged with an average altitude of approximately 2000 m and 1100 m, respectively [*Liu and Dong, 2013; Yang et al., 2010*]. **(Appendix A)**. The climate of the YP is characterized by a higher mean annual temperature (MAT) of 13 °C ~ 20 °C and a lower mean annual precipitation (MAP) of 600 ~ 900 mm/yr [*Tong et al., 1994*] than the GP characterized by a MAT of 12 °C ~ 16 °C and a MAP of 800 ~ 1200 mm/

yr [*Liu and Xiong et al., 2015*]. The opposite trends in MAT and MAP enlarge the difference in the RH between the YP and GP from 50% to 85% [*Xu, 1991*]. Moreover, it is near the climatic inflection point that controls soil reddening and yellowing, as proposed in our previous studies [*Long et al., 2016*]. As a result, the saprolitic soils derived from the widespread Triassic carbonate rocks [*Feng, 2005*] have demonstrated a common reddening trend (3.2 YR ~ 6.3 YR) in the YP due to its lower RH from 58% to 73% while the soils have demonstrated a significant yellowing trend (6.2 YR ~ 9.6 YR) in the GP due to its high RH from 79% to 82%.

We collected two saprolitic soil profile sequences from the YP and GP that are separated by the boundary of the Wumeng Mountains. The profiles of YP1, YP2 and YP3 were collected from the YP under increasing MAT from 13.4 °C to 18.2 °C and decreasing MAP from 924 mm/yr to 762 mm/yr. Similarly, the profiles of GP1, GP2 and GP3 were collected under slowly increasing MAT from 12.9 °C to 14.4 °C and a decreasing MAP from 937 mm/yr to 899 mm/yr. These profiles were collected on the local highland and were covered by natural vegetation ranging from herbaceous plants in YP to evergreen forests in GP. The soil type in the YP can be categorized as an Acrisol, while that in the GP can be categorized as an Alisol [*IUSS Working Group WRB, 2015*]. The soil samples were collected from the surface to the bottom of the outcrops at intervals of 20 cm or 40 cm covering the main horizons depending on the thickness of the outcrops.

2.2 Chemical and physical measurement

The air-dried samples were sieved by a 2-mm sieve and ground into powder for chemical analysis. The chemical compositions were determined with an ARL9800XP + X-ray spectrophotometer and have been expressed as oxides. The chemical weathering index (CIA) was calculated as the molar percentage of Al_2O_3 / (Al_2O_3 + CaO + Na_2O + K_2O) [*Nesbitt and Young, 1982*], and the *S*a index was calculated as the molar ratio of SiO_2/Al_2O_3 [*Bayan and Ruxton, 1968*]. Free iron (Fe_d) and amorphous iron (Fe_o) were extracted by the citrate-bicarbonate-dithionate (CBD) method [*Mehra and Jackson, 1960*] and ammonium oxalate method [*Schwertmann, 1964*], respectively.

The diffuse reflectance spectra (DRS) were measured with a Perkin Elmer Lambda 900 UV/VIS/NIR spectrometer at 2 nm intervals. The standard Hm and Gt minerals used in the experiment were the Pfizer R1599 pure red from Pfizer Company and Synox HY610 pure yellow nanoscale iron oxides from the Hoover Color Corporation. The redness was calculated according to the ratio of mean reflectance between the red-light band (630 ~ 700 nm) and the visual light band (400 ~ 700 nm) [*Judd and Wyszecki, 1975*]. The Hm content was estimated using a working curve established by the sample substrate after CBD treatment mixed with a series of standard Hm and Gt samples in different ratios [*Long et al., 2011, 2016*]. Finally, we assigned Fe_d to be the combination of Fe in stoichiometric Hm, Gt [*Torrent et al., 2007*] and Fe_o, and the contents of Hm and Gt were calculated by the following equation:

$$\text{Hm (g kg}^{-1}) = 0.0012\times e^{0.227 * \text{Redness}}$$

$$\text{Gt (g kg}^{-1}) = 1.59 \times (Fe_d - Fe_o - \text{Hm}/1.43)$$

The magnetic susceptibility of all samples was measured in the laboratory at 0.47 kHz (χ_{lf}) and 4.7 kHz (χ_{hf}) with a Bartington MS2B susceptibility meter. The frequency-dependent susceptibilities χ_{fd} and $\chi_{fd}\%$ representing the absolute and relative contributions of SP particles were calculated as $\chi_{lf} - \chi_{hf}$ and $(\chi_{lf} - \chi_{hf})/\chi_{lf} \times 100\%$, respectively [*Dearing et al., 1996; Worm, 1998*]. Meanwhile, the anhysteretic remanent magnetization (ARM) was imparted using a peak of the 100 mT alternating field and a 0.05 mT biasing field with a Molspin demagnetizer [*Dunlop and Özdemir,1997*]. The χ_{ARM} parameter was calculated by the ARM and normalized by the biasing field. The saturation isothermal remanent magnetization (SIRM) was attained at 1 T with the ASC-10 impulse magnetizer, and all the remanence magnetizations were measured in the AGICO JR6 spinner magnetometer. HIRM was calculated by $(IRM_{-300mT} + SIRM)/2$, which mainly reflects the content changes of high-coercivity minerals, such as Hm [*Nie et al., 2010*], and the *S-ratio* is calculated by $-IRM_{-300mT}/SIRM$ [*King et al., 1991*], which indicates the relative abundance of the FM to AFM minerals [*Thompson and Oldfield, 1986; Liu et al., 2007*].

3. Results

As illustrated in **Figure 1**, the change of Fe_d/Fe_t is comparable in both sequences. In contrast, the Hm/(Hm+Gt) demonstrates a significant shift from 0.20 to 0.98 in the YP sequence but remains low from 0.05 to 0.19 in the GP sequence **(Figure 1a)**. In addition, the Fe_o content is also little higher in the YP sequence than those in the GP sequence. However, the Hm content in the YP sequence is much higher than that in the GP sequence **(Figure 1b)**. Correspondingly, the χ_{lf} ranges from 573.9×10^{-8} m^3 kg^{-1} to 4005.1×10^{-8} m^3 kg^{-1} in the YP sequence, which is much higher than that ranging from 8.7×10^{-8} m^3 kg^{-1} to 310.5×10^{-8} m^3 kg^{-1} in the GP sequence **(Figure 1c)**. More importantly, χ_{lf} changes in phase with redness control by Hm in the YP sequence but out of phase in the GP sequence. The χ_{fd}, χ_{ARM} and SIRM, also exhibit synchronous changes with χ_{lf} (**Figure 2a-2c**), although the χ_{fd}%, χ_{fd}/χ_{ARM}, ARM/SIRM are more comparable across both sequences (**Figure 2e-2g**). χ_{fd}% and ARM/SIRM are only slightly higher in the YP sequence, while χ_{fd}/χ_{ARM} is slightly higher in the GP sequence. In addition, the HIRM is higher in the YP sequence than that in the GP sequence **(Figure 2d)**, but it has a less correlation with the increasing χ_{lf}. The *S-ratio* exhibits a rapid increase with increasing χ_{lf} in the GP sequence but remains close to 1 in the YP sequence **(Figure 2h)**.

4. Discussion

4.1 Comparable chemical weathering and significant iron oxides transformation driven by opposite climate transitions

Theoretically, the increasing of rainfall and temperature favors chemical weathering and the enrichment of iron oxides because primary iron-bearing minerals are often preferentially weathered to form secondary iron oxides [*Kump et al., 2000*]. However, in the GP under the wet and cool climate, the higher rainfall is superimposed by lower evaporation. Although the changed leaching could be enhanced by the more effective rainfall, the chemical reaction rates should be retarded by the lowering temperature [*Kump et al., 2000; White and Blum, 1995*]. The phenomena can be widely observed in mountainous, where the rainfall also accompanied by the inverse change of the temperature [*Long et al., 2016*]. Nevertheless, the effective rainfall would favor the formation of iron oxyhydroxides such as Gt [*Schwertmann, 1971*]. However, in the YP under the dry and warm climate, the lower rainfall superimposed by the increased evaporation retards chemical leaching but promotes the dehydration of amorphous iron oxides to form iron oxides like Hm and Mgh [*Schwertmann, 1971; Barrón and Torrent, 2002; Grogan et al., 2003*]. Generally, these inverse changes of temperature with rainfall lead to less variability in chemical weathering intensity and more significant differentiation of iron oxides indicated by Hm/(Hm+Gt) in both sequences.

4.2 Coordination and competition between FM and AFM particles driven by opposite climate transitions

The magnetic properties revealed a common positive correlation with Fe_o in both sequences except that the SIRM and HIRM reveals more consistent correlation with Fe_o (**Figures 3a-3e).** Although the contents of Hm and FM particles are much higher in the YP sequence than these in the GP sequence **(Figures 3f-3j)**. However, the Hm and FM particles change in phase in the YP sequence but out of phase in the GP sequence **(Figures 3f-3i)** except that the HIRM reveals more consistent correlation with Hm **(Figure 3j)**. Moreover, the χ_{fd}/χ_{ARM}, χ_{lf}/χ_{ARM} in the GP soils **(Figures 3l-3m),** as well as the χ_{fd}%, χ_{fd}/χ_{ARM} and ARM/SIRM in the YP soils, which indicate the ratio of fine FM particles to coarser FM particles both decrease with Hm in both sequences **(Figures 3k-3n).** However, the *S-ratio* reveals significant decreasing with Hm in the GP yellowing soils but remains constant in the YP reddening soils **(Figure 3o)**.

These outcomes verify the FM particles with growing size as the intermediate products of AFM Hm aging from amorphous iron oxides [*Barrón and Torrent, 2002*] but the correlation between FM particles and Hm depends on Hm/(Hm+Gt) controlled by RH [*Torrent et al., 2006; Long et al., 2015*]. The positive correlation between FM particles and Hm, as revealed in the YP reddening soils, occurs under the condition with a high formation efficiency of Hm, indicate by Hm/(Hm+Gt) from 0.20 to 0.98 under the low RH. It is consistent with the result revealed in aerobic soils with high Hm/(Hm+Gt) [*Torrent et al., 2006*], especially in the red Ferralsols derived from basalt with the Hm/(Hm+Gt) above 0.6 [*Long et al., 2015*]. However, the negative correlation between Hm and FM particles, as revealed in the GP yellowing soils, occurs under the conditions with a low Hm/(Hm+Gt) from 0.05 to 0.19 under high RH. These negative correlations can be observed in each profile of the GP sequence **(Figure 1c)**. This result apparently accords with the yellow soils derived from the downslope of a subtropical granitic toposequence, with Hm/(Hm+Gt) < 0.2 and Hm% <1% controlled by the downward increasing of water activity [*Guo et al., 2021*].

However, in contrast to the topsequence affected by the dynamic migration of magnetic particles [*Guo et al., 2021*]. The negative correlation between FM particles and Hm in the climosequence of the GP under high RH indicates there would be a competition between FM particles and Hm since high soil water activity retards the formation of iron oxides but promote the formation of iron oxyhydroxides [*Tardy and Nahon, 1985; Trolard and Tardy, 1987*]. Moreover, with the slow increasing of RH from GP1 to GP3, a little amount of FM particles has accumulated at the cost of Hm. The outcome confirms the FM particles as rainfall indicator while the Hm as temperature or evaporation indicator at a large scale [*Gao et al., 2018*]. If the different aging processes under aerobic conditions in natural systems of Hm and Gt from Fh are combined as $\mathrm{Gt} \xleftarrow{1} \mathrm{Fh} \xrightarrow{2} \mathrm{SP\ Mgh} \xrightarrow{3} \mathrm{SD\ Mgh} \xrightarrow{4} \mathrm{Hm}$ [*Schwertmann, 1971; Barrón and Torrent, 2002*], in the wet and cool climate transition, the step 1 and step 2 are favored, which results in the accumulation of a large amount of Gt and a limited number of FM particles at the cost of previously formed Hm. However, in the dry and warm climate transition with low RH, the step 3 and step 4 are favored, which results in the accumulation of a large number of FM particles, as well as their significant grain growth and transformation into Hm.

4.3 Significance in paleoclimate cycle and pattern reconstruction

In both sequences under high and low RH, an increase in rainfall is often accompanied by decreasing temperature. It could help us understand the response of iron oxide to extreme dry-wet cycles and patterns. In paleoclimate reconstruction, changes in rainfall are often considered to be accompanied by synchronous changes in temperature [*Liu et al., 2001, 2012*; *Kukla, 1987; Maher, 1998, 2016*]. This climate pattern could lead to remarkable changes in the Fe_d content controlled by chemical weathering that constrains the changes in the Hm/(Hm+Gt) controlled by RH [*Ji et al., 2004; Balsam et al., 2004; Ding et al., 2001*]. However, if the temperature and rainfall changes in opposing directions, a significant change in Hm/(Hm+Gt) can be observed, and the formation efficiency of Hm and FM particles and their correlation could change, resulting in the mismatching of color indices and magnetic properties. Actually, the magnetism and redness are often coupled in loess deposits under dry and cool climates [*Ji et al.,2004*], but they are frequently observed as decoupled in paleosols under warm and wet climate, with Hm/(Hm+Gt) commonly decreasing below 0.2 [*Ji et al., 2004; Hao et al., 2009*]. This phenomenon agrees with the competition occurring between Hm and FM particles under the high RH present in the GP sequence with low Hm/(Hm+Gt). In addition, the change content of FM particles estimated by χ_{lf} (approximately 30×10^{-8} m^3 kg^{-1} ~ 190×10^{-8} m^3 kg^{-1}) [*Ji et al., 2004*] well matches the content changes in the hematite content (approximately 0.1% ~ 0.2%) [*Guo et al., 2021; Ji et al., 2004*] if the χ_{lf} of pure FM particles are estimated around 110, 000×10^{-8} m^3 kg^{-1} [*Worm and Jackson, 1999*].

However, in some warm stages, such as red clays with Hm/(Hm+Gt) above 0.6 [*Hao et al., 2009*], uncertain and even opposite correlation between redness and magnetism were also found [*Ding et al., 2001; Nie et al., 2008; Hu et al., 2009*]. In the YP sequence as well as red Ferrosols with high Hm/(Hm+Gt) under low RH and high evaporation, the positive correlation between FM particles and Hm still remains although the formation of fine FM particles are observed to deaccelerate with Hm [*Long et al., 2015*]. Therefore, the opposite correlation between redness and magnetism in Tertiary Red Clay could also correlate with the increased iron crystallinity with longer aging time [*Hu et al., 2009; Jiang et al., 2018*], less ligand protection of highly weathering soils [*Ren et al., 2020*] in addition to high Hm/(Hm+Gt). Nevertheless, it verifies the magnetic parameters indicating the ratios of different FM particles could be more reasonable than the magnetic parameters indicating the contents of magnetic particles in paleoclimate reconstruction under widely climate scale [*Nie et al., 2014*].

In addition, it should be noted that the soil sequences exhibit comparable changes in the Fe_d contents but significant changes in the Hm/(Hm+Gt). The higher redness and degree of magnetism are observed in the YP sequence under dry and warm climate. In contrast, under comparable changes in rainfall and temperature on the CLP, the Fe_d of the paleosols is often two times that of loesses [*Ding et al., 2001*], while the Hm/(Hm+Gt) is slightly lower in paleosols [*Ji et al.,2004*]. The higher redness and degree of magnetism are observed in paleosols formed under a wet and warm climate. Since the soil reddening and magnetic enhancement could be achieved by the dehydration of iron oxides associated with strong evaporation [*Barrón and Torrent, 2002; Long et al., 2015*] even when chemical weathering is restrained by low rainfall. The accompanying change in temperature should be considered as important as rainfall in paleoclimate reconstruction, especially under extreme climate cycles and patterns shifts.

5. Conclusion

To unravel the changing relationship between AFM and FM particles and their climatic implications under extremely climate, we examined two soil sequences in the YP and GP on the eastern edge of TP. The YP and GP sequences have undergone significant reddening and yellowing, respectively, as a result of dry and wet climate transitions accompanied by inverse changes in temperature and rainfall. The AFM Hm and FM particles are much more enriched in the YP reddening soils than these in the GP yellowing soils although the change in total amount of iron oxides controlled by chemical weathering are comparable. The dry and warm climate favors the dehydration of amorphous iron oxides to form higher contents of AFM Hm and FM particles, while the wet and cool climate impedes their formation and leads to competition. The little amount of FM particles could form at the cost of previously formed Hm under high RH. The model well interprets the synchronous and asynchronous changes in color and magnetism under the dry and wet cycles, and suggests that evaporation is as important as precipitation in extreme paleoclimate reconstruction based on iron oxides.

Acknowledgments

We thank Dr Ren Juan and Xing Dengchun for their help in the laborious field work in Southwest China. This study was co-supported by the National Natural

Science Foundation of China (41877369) and the Natural Science Foundation of Chongqing, China (CSTC2018JCYJAX0456). The original data presented in this paper can be accessed through the public domain repository Zenodo at http://doi.org/10.5281/zenodo.4495880

Appendix A: **(a)** Location of sampling points on the YP and GP; **(b)** The YP is characterized by higher elevation and lower RH than the GP. The profiles of YP1, YP2, YP3 and GP1, GP2, GP3, with increasing relative humidity in the sequences were sampled in the YP and GP, respectively.

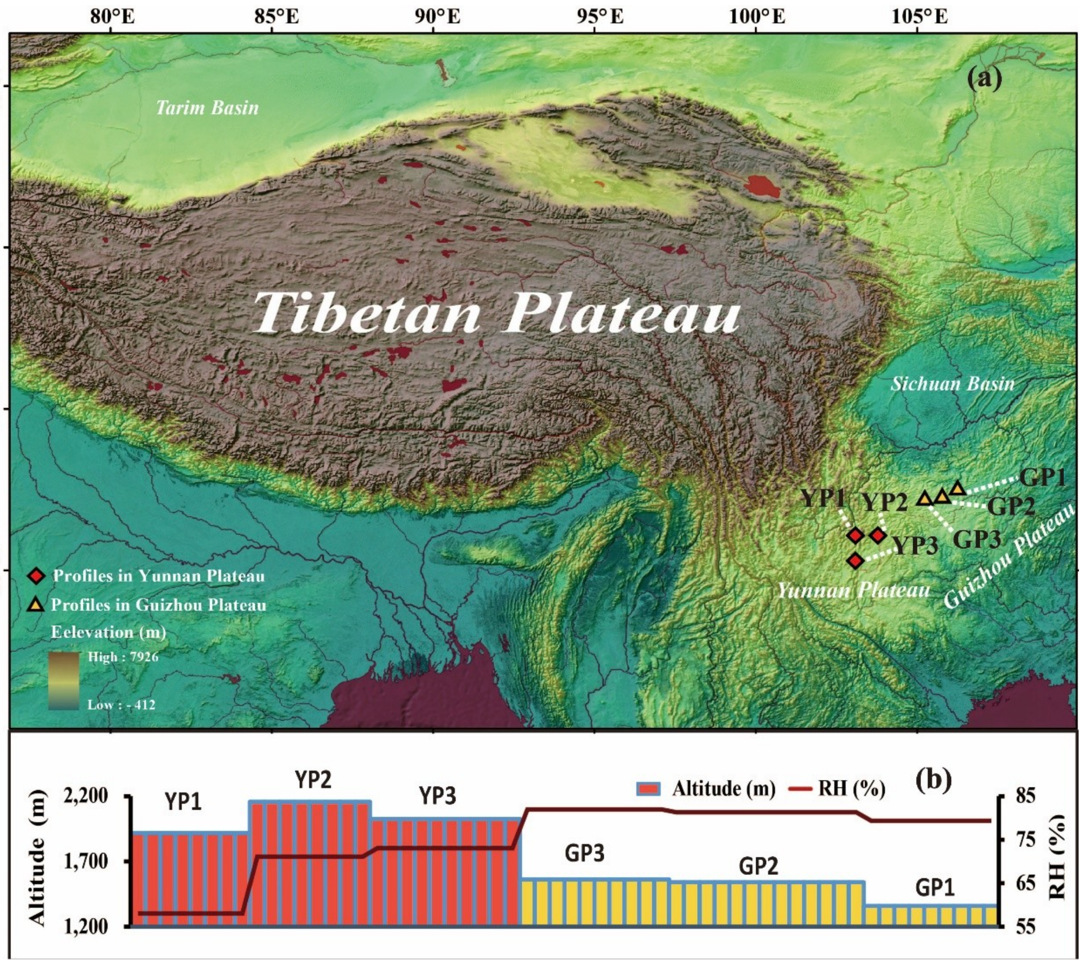

Figure 1. The Fe_d/Fe_t keeps comparable in both sequences but the Hm/(Hm+Gt) is much higher in the YP sequence than that in the GP sequence **(a)**. The Fe_o in the YP sequence is a little higher than that in the GP sequence while the Hm is significantly higher in the YP than that in the GP **(b)**. The magnetic susceptibility changes in phase with the redness in the YP sequence but out of phase in the GP sequence **(c)**. Note that the Fe_o, Hm and χ_{lf} are shown in logarithmic form because of the significant difference between profiles.

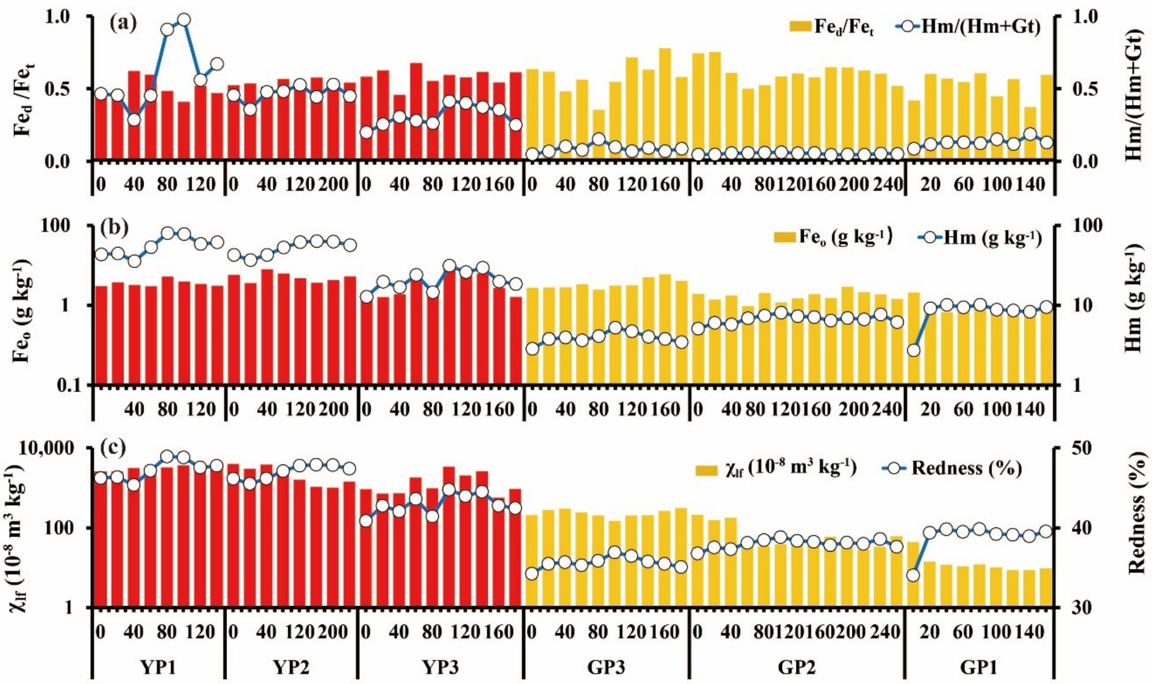

Figure 2. The χ_{fd}, χ_{ARM} and SIRM generally increase with χ_{lf} **(a-c)** except the HIRM **(d)**. The χ_{fd}%, χ_{fd}/χ_{ARM}, ARM/SIRM demonstrates no systematical trend in the GP sequence but demonstrates decreasing in the YP sequence except for χ_{fd}/χ_{ARM} **(e-g)**. However, the *S-ratio* demonstrates a significant increase with χ_{lf} in the GP sequence but a slower increase in the YP sequence **(h)**.

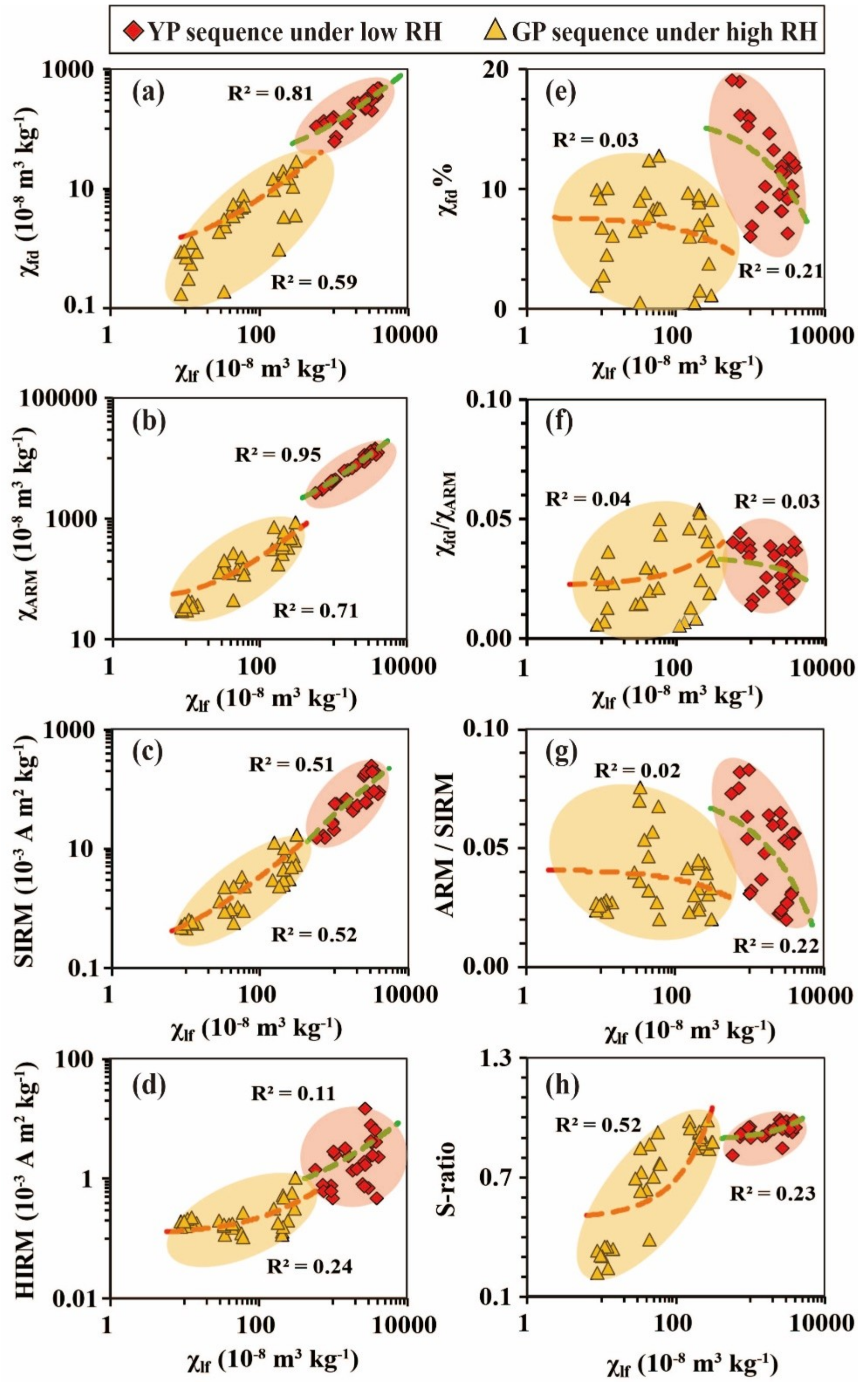

Figure 3. The magnetic parameters generally increase with Fe_o **(a-e)**. Both the FM particles and Hm are more enriched in the YP than that in the GP but they change in phase in the YP and out of phase in GP except for the HIRM **(f-j)**. The χ_{fd}/χ_{ARM}, χ_{lf}/χ_{ARM} decreases with Hm in the GP while $\chi_{fd}\%$, χ_{fd}/χ_{ARM} and ARM/SIRM decreases with Hm in the YP and the *S-ratio* reveals significant decreasing with Hm in the GP but remains constant in the YP **(k-o)**.

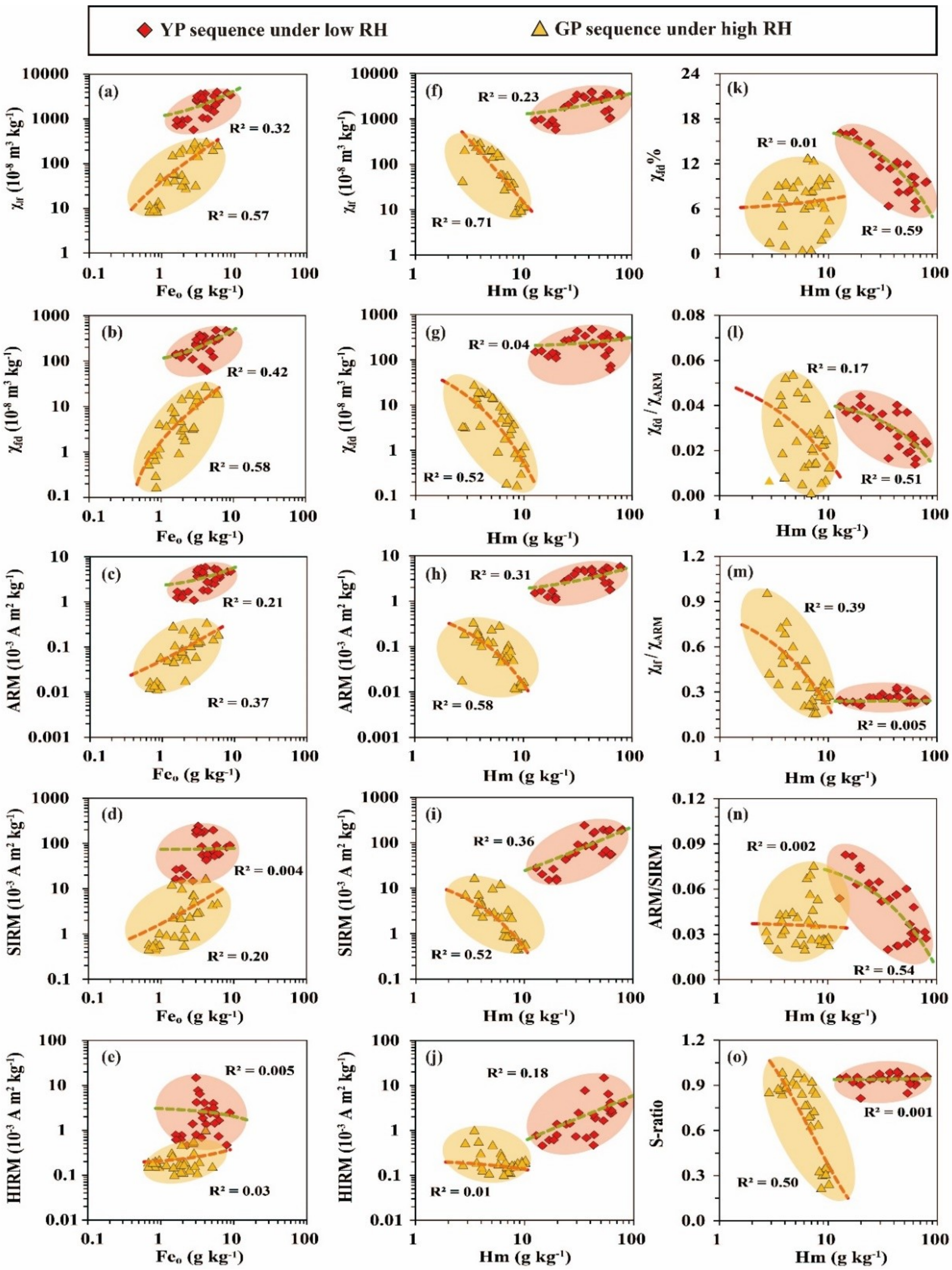

Reference

Balsam, W., Ji, J.F., and J. Chen (2004). Climatic interpretation of the Luochuan and Lingtai loess sections, China, based on changing iron oxide mineralogy and magnetic susceptibility, *Earth and Planetary Science Letters*, *223*(3-4), 335-348. https://doi.org/10.1016/j.epsl.2004.04.023

Bao, X., Sun, X., Xu, M., Eaton, D.W., Song, X., Wang, L., Ding, Z.H., Mi, N., Li, H., Yu, D.Y., Huang, Z.C., and P. Wang (2015). Two crustal low-velocity channels beneath se Tibet revealed by joint inversion of Rayleigh wave dispersion and receiver functions, *Earth and Planetary Science Letters*, *415*, 16-24. https://doi.org/10.1016/j.epsl.2015.01.020

Barrón, V., and J. Torrent (2002). Evidence for a simple pathway to maghemite in Earth and Mars soils, *Geochimica Et Cosmochimica Acta*, *66*(15), 2801-2806. https://doi.org/10.1016/S0016-7037(02)00876-1

Barrón, V., Torrent, J., and E.de Grave (2003). Hydromaghemite, an intermediate in the hydrothermal transformation of 2-line ferrihydrite into hematite, *American Mineralogist*, *88*(11-12), 1679-1688. https://doi.org/10.2138/am-2003-11-1207

Bayan, P., and Ruxton (1968). Measures of the degree of chemical weathering of rocks, *Journal of Geology*, *76*, 518-827. http://www.jstor.org/stable/30066179

Chlachula, J. (2003). The Siberian loess record and its significance for reconstruction of Pleistocene climate in north-Central Asia, *Quaternary Science Reviews*, *22*(18-19), 1879-1906. https://doi.org/10.1016/S0277-3791(03)00182-3

Christensen, P.R., Morris, R.V., Lane, M.D., Bandfield, J.L., and M.C. Malin (2001). Global mapping of Martian hematite mineral deposits: Remnants of water-driven processes on early Mars, *Journal of Geophysical Research Planets*, *106*(E10). https://doi.org/10.1029/2000JE001415

Cornell, R.M., and U. Schwtermann (2003). The Iron Oxides: Structure, properties, reactions, occurrences and uses, Wiley-VCH Verlag GmbH & Co. KGaA, Weinheim, 435-437

Dearing, J.A., Hay, K.L., Baban, S.M.J., Huddleston, A.S., Wellington, E.M.H., and P.J. Loveland (1996). Magnetic susceptibility of soil: an evaluation of conflicting theories using a national data set, *Geophysical Journal International*, *127*(3), 728-734. https://doi.org/10.1111/j.1365-246X.1996.tb04051.x

Dearing, J.A., Dann, R.J.L., Hay, K., Less, J.A., Loverland, P.J., Maher, B.A., and K. O'Grady (1996). Frequency-dependent susceptibility measurements of environmental materials, *Geophysical Journal International*, *124*, 228–240. https://doi.org/10.1111/j.1365-246X.1996.tb06366.x

Ding, Z.L., Yang, S., Sun, J., and T. Liu (2001). Iron geochemistry of loess and red clay de-posits in the Chinese Loess Plateau and implications for long-term Asian

monsoon evolution in the last 7.0 Ma, *Earth and Planetary Science Letters*, *185*(1-2), 99-109. https://doi.org/10.1016/S0012-821X(00)00366-6
Ding, Z. L., Ranov, V., Yang, S. L., Finaev, A., Han, J. M., and G. A. Wang (2002). The loess record in southern Tajikistan and correlation with Chinese loess, *Earth and Planetary Science Letters*, *200*(3-4), 387-400. https://doi.org/10.1016/S0012-821X(02)00637-4
Dunlop, D. J., and Ö. ÖZdemir (1997). Rock magnetism fundamentals and frontiers. Cambridge studies in magnetism series. xxi + 573 pp. Cambridge, New York, Port Chester, Melbourne, Sydney: Cambridge University press. *Geological Magazine*, *135*, 287-300.
Feng, J. L. (2004) Provenance of Terra Rossa on the carbonate rocks in Yunnan-Guizhou Plateau, China, Institute of Geographic Science and Natural Resources Research, CAS. http://ir.igsnrr.ac.cn/handle/311030/368
Gao, X.B., Hao, Q.Z., Wang, L., Oldfield, F., Bloemendal, J., Deng, C.L., Song, Y., Ge, J.Y., Wu, H.B., Li, F.J., Han, L., Fu, Y., and Z.T. Guo (2018). The different climatic response of pedogenic hematite and ferrimagnetic minerals: Evidence from particle-sized modern soils over the Chinese Loess Plateau, *Quaternary Science Reviews*, *179*, 69-86. https://doi.org/10.1016/j.quascirev.2017.11.011
Grogan, K.L., Gilkesl, R.J., and B.G. Lottermoser (2003). Maghemite Formation in Burnt Plant Litter at East Trinity, North Queensland, Australia, *Clays and Clay Minerals*, *51*(4), 390-396.https://doi.org/doi: 10.1346/CCMN.2003.0510404
Guo, S.L., Cai, Y.F., Ren, J., Guan, Y.X., Xin, D.C., and X.Y. Long (2021). Formation and migration of magnetic particles associated with iron oxide transformation at a hillslope scale, *Catena*, *197*. https://doi.org/10.1016/j.catena.2020.104944
Guo, X.L., Liu, X.M., Li, P.Y., Lü, B., Guo, H., Qu, C., Liu, Z., and M.M. Ma (2013). The magnetic mechanism of paleosol S5 in the Baoji section of the southern Chinese Loess Plateau, *Quaternary International*, *306*, 129-136. https://doi.org/10.1016/j.quaint.2013.02.033
Han, J.M., Lü, H.Y., Wu, N.Q., and Z.T. Guo (1996). The magnetic susceptibility of modern soils in China and its use for paleoclimate reconstruction, *Studia Geophysica et Geodaetica*, *40*, 262–275. https://doi.org/10.1007/BF02300742
Hao, Q. Z., Oldfield, F., Bloemendal, J., Torrent, J., and Z. T. Guo (2009). The record of changing hematite and goethite accumulation over the past 22 Myr on the Chinese Loess Plateau from magnetic measurements and diffuse reflectance spectroscopy, *Journal of Geophysical Research*, *114*(B12), 465-484. http://doi.org/ 10.1029/2009JB006604.
Heller, F., Liu, X.M., Liu, T.S., and T.C. Xu (1991). Magnetic susceptibility of loess in China, *Earth and Planetary Science Letters*, *103*, 301-310. https://doi.org/10.1016/0012-821X(91)90168-H
Heller, F., and Liu T.S. (2010). Magnetism of Chinese loess deposits, *Geophysical Journal of the Royal Astronomical Society*, *77*(1), 125-141.

https://doi.org/10.1111/j.1365-246X.1984.tb01928.x

Hu, P. X., Liu, Q. S., J. Torrent, V. Barrón, and C.S. Jin (2013), Characterizing and quantifying iron oxides in Chinese loess/paleosols: implications for pedogenesis, *Earth and Planetary Science Letters*, *369-370*(3), 271-283. https://doi.org/10.1016/j.epsl.2013.03.033

Hu, X.F., Wei, J., Xu, L.F., Zhang, G.L., and W.G. Zhang (2009). Magnetic susceptibility of the Quaternary red clay in subtropical China and its paleoenvironmental implications, *Palaeogeography, Palaeoclimatology, Palaeoecology, 279*(3-4), 216-232. https://doi.org/10.1016/j.palaeo.2009.05.016

Hu, X.F., L.F. Xu, Y. Pan, and M.N., Shen (2009). Influence of the aging of Fe oxides on the decline of magnetic susceptibility of the Tertiary red clay in the Chinese Loess Plateau, *Quaternary International*, *209*(1-2), 22-30. https://doi.org/10.1016/j.quaint.2009.02.019

IUSS Working Group WRB (2015). World reference base for soil resources 2014, update 2015, International soil classification system for naming soils and creating legends for soil maps. World Soil Resources Reports 106, 144-146pp., Food and Agriculture Organization of the United Nations, FAO, Rome.

Ji, J.F., W. Balsam, and J. Chen (2001). Mineralogic and climatic interpretations of the Luochuan loess section (China) based on diffuse reflectance spectrophotometry, *Quaternary Research*, *56*(1), 23-30. https://doi.org/10.1006/qres.2001.2238

Ji, J.F., Chen, J., Balsam, W., Lu, H.Y., Sun, Y.B., and H.F. Xu (2004). High resolution hematite/goethite records from Chinese loess sequences for the last glacial-interglacial cycle: rapid climatic response of the East Asian Monsoon to the tropical Pacific, *Geophysical Research Letters*, *31*(3), L03207. https://doi.org/ 10.1029/2003GL018975

Jiang, Z.X., Q.S. Liu, A.P. Roberts, V. Barrón, J. Torrent, and Q. Zhang (2018). A new model for transformation of ferrihydrite to hematite in soils and sediments, *Geology*, *46*(11), 987-990. https://doi.org/10.1130/G45386.1

Judd, D.B., and G. Wyszecki (1975). Color in Business, Science, and Industry, 553 pp., John Wiley, New York

King, J.W., and J.E.T. Channel (1991). Sedimentary magnetism, environmental magnetism, and magnestostratigrapgy, *Reviews of Geophysics*, *29*, 358-370. https://doi.org/10.1002/rog.1991.29.s1.358

Kukla, G. (1987). Loess stratigraphy in central China, *Quaternary Science Reviews*, *6*(3-4), 209-219. https://doi.org/10.1016/0277-3791(87)90004-7

Kump, L.R., Brantley, S.L., and M.A. Arthur (2000). Chemical weathering, atmospheric CO_2, and climate, *Annual Review of Earth and Planetary Sciences, 28* (1), 611-667. https://doi.org/10.1146/annurev.earth.28.1.611

Li, G.J., Chen, J., Ji, J.F., Yang, J.D., and T.M. Conway (2009). Natural and anthropogenic sources of East Asian dust, *Geology*, *37,* 727-730. https://doi.org/10.1130/G30031A.1

Li, J., and X.M. Fang (1999). Uplift of the Tibetan Plateau and environmental changes, *Chinese Science Bulletin*, *44*, 2117–2124 https://doi.org/ 10.1007/ BF

03 182692

Liu, C.C., and C.L. Deng (2012). Magnetic mineralogy of the red soil sequences in southern China and its variety, *Quaternary. Science*, *32*(4), 626-634. https://doi.org/10.3969/j.issn.1001-7410.2012.04.07

Liu, Q.S., Bloemendal, J., Torrent, J., and C.L. Deng (2006). Contrasting behavior of hematite and goethite within paleosol S5 of the Luochuan profile, Chinese Loess Plateau, *Geophysical Research Letters*, *33*(20), L20301. https://doi.org/10.1029/2006GL027172

Liu, Q.S., Deng, C.L., Torrent, J., and R.X. Zhu (2007). Review of recent developments in mineral magnetism of the Chinese loess, *Quaternary Science Reviews*, *26*(3-4), 368-385. https://doi.org/10.1016/j.quascirev.2006.08.004

Liu, Q.S., Roberts, A.P., Torrent, J., C.S. Horng, and J. Larrasoaña (2007b). What do the HIRM and *S-ratio* really measure in environmental magnetism? *Geochemistry Geophysics Geosystems*, *80*(9). https://doi.org/ 10.1029/2007GC001717

Liu, T.S., and Z.L. Ding (2003). Chinese loess and paleomonsoon, *Annual Review of Earth and Planetary Sciences*, *26*(1), 111-145. https://doi.org/10.1146/annurev.earth.26.1.111

Liu, X.D., and B.W. Dong (2013). Influence of the Tibetan Plateau uplift on the Asian monsoon-arid environment evolution, *Chinese Science Bulletin*, *58*, 4277–4291, https://doi.org/10.1007/s11434-013-5987-8

Liu, X.M., T. Rolph, J. Bloemendal, J.S., and T.S. Liu (1995). Quantitative estimates of palaeoprecipitation at Xifeng, in the Loess Plateau of China, *Palaeogeography, Palaeoclimatology, Palaeoecology*, *113*(2-4), 243-248. https://doi.org/10.1016/0031-0182(95)00053-o

Liu, X.M., Hesse, P., J. Begét, and T. Rolph (2001). Pedogenic destruction of ferrimagneticsin Alaskan loess deposits, *Australian Journal of Soil Research*, *39*(1), 99-115. https://doi.org/10.1071/SR99081

Liu, X.M., T. Rolph, Z. An, and P. Hesse (2003). Paleoclimatic significance of magnetic properties on the Red Clay underlying the loess and paleosols in China, *Palaeogeography, Palaeoclimatology, Palaeoecology*, *199*(1-2), 153-166. https://doi.org/10.1016/S0031-0182(03)00504-2

Liu, X.M., Liu, Z., Lü, B., S.B. Markovic, Chen, J.S., Guo, H., Ma, M., Zhao, G.Y., and H. Feng (2012). The magnetic properties of Serbian loess and its environmental significance, *Chinese Science Bulletin*, *57*(33), 3173-3184. https://doi.org/10.1007/s11434-012-5383-9

Long, X.Y., J.F. Ji, and W. Balsam (2011). Rainfall-dependent transformations of iron oxides in a tropical saprolite transect of Hainan Island, South China: Spectral and magnetic measurements, *Journal of Geophysical Research-Earth Surface*, *116*, F03015. https://doi.org/10.1029/2010jf001712

Long, X.Y., J.F. Ji, W. Balsam, V. Barrón, and J. Torrent (2015). Grain growth and transformation of pedogenic magnetic particles in red Ferralsols, *Geophysical Research Letters*, *42*(14), 5762-5770.

https://doi.org/10.1002/2015gl064678

Long, X.Y., J.F. Ji, V. Barrón, and J. Torrent (2016). Climatic thresholds for pedogenic iron oxides under aerobic conditions: Processes and their significance in paleoclimate reconstruction, *Quaternary Science Reviews*, *150*, 264-277. https://doi.org/10.1016/j.quascirev.2016.08.031

Lu, H.Y., Stevens, T., Yi, S.W., and X.F. Sun (2006). An erosional hiatus in Chinese loess sequences revealed by closely spaced optical dating, *Chinese Science Bulletin*, *51*, 2253–2259. https://doi.org/10.1007/s11434-006-2097-x

Maher, B.A. (1998). Magnetic properties of modern soils and Quaternary loessic paleosols, paleoclimatic implications, *Palaeogeography, Palaeoclimatology, Palaeoecology*, *137*(1-2), 25–54. https://doi.org/10.1016/S0031-0182(97)00103-X

Maher, B.A. (2016). Palaeoclimatic records of the loess/palaeosol sequences of the Chinese loess plateau, *Quaternary Science Reviews*, 154, 23-84. https://doi.org/10.1016/j.quascirev.2016.08.004

Maxbauer, D.P., Feinberg, J.M., and Fox, D.L. (2016). Magnetic mineral assemblages in soils and paleosols as the basis for paleoprecipitation proxies: a review of magnetic methods and challenges, *Earth-Science Reviews*, *155*, 28-48. https://doi.org/10.1016/j.earscirev.2016.01.014

Mehra, O.P., and M.L. Jackson (1960). Iron oxide removal from soils and clays by a dithionite-citrate system buffered with sodium bicarbonate, *Clays and Clay Minerals, 7*, 317-327. https://doi.org/10.1016/B978-0-08-009235-5.50026-7

Nesbitt, H.W., and G. Young (1982). Early Proterozoic climates and plate motions inferred from major element chemistry of lutites, *Nature*, *299*(5885), 715-717. https://doi.org/10.1038/299715a0

Nesbitt, H.W., Young, G.M., Mclennan, and S.M., R.R. Keays (1996). Effects of chemical weathering and sorting on the petrogenesis of siliciclastic sediments, with implications for provenance studies, *Journal of Geology*, *104*(5), 525-542. https://doi.org/10.1086/629850

Nie, J.S., King, J.W., and X.M. Fang (2008). Link between benthic oxygen isotopes and magnetic susceptibility in the red-clay sequence on the Chinese loess plateau, *Geophysical Research Letters*, *35*(3), L03703. http://ir.itpcas.ac.cn/handle/131C11/761

Nie, J.S., Song, Y.G., King, J. W., Fang, X.M., and C. Heil (2010). HIRM variations in the Chinese red-clay sequence: insights into pedogenesis in the dust source area, *Journal of Asian Earth Sciences*, *38*(3-4), 96-104. https://doi.org/10.1016/j.jseaes.2009.11.002Get rights and content

Nie, J.S., Song, Y.G., King, J., and R. Zhang (2013). Six million years of magnetic grain-size records reveal that temperature and precipitation were decoupled on the Chinese Loess Plateau during 4.5–2.6 Ma, *Quaternary Research*, *79*, 465–470. https://doi.org/10.1016/j.yqres.2013.01.002

Nie, J.S., Stevens, Thomas, Song, Y.G., J.W. King, Zhang, R., Ji, S.C., Gong, L.S., and D.S. Cares (2014). Pacific freshening drives Pliocene cooling and Asian monsoon intensification, *Scientific Reports*, *4*, 5474. https://doi.org/10.1038/srep05474

Nie, J.S., Song Y.G., and J.W. King (2016). A review of recent advances in Red-Clay environmental magnetism and paleoclimate history on the Chinese Loess Plateau, *Frontiers in Earth Science*, *4*(27), 1-13. https://doi.org/10.3389/feart.2016.00027

Pan, B.T., Gao, H.S., Li, B.Y., and J.J. Li (2004). Step-like landforms and uplift of the Qinghai-Xizang Plateau, *Quaternary Sciences*, *24*(1), 50-57. https://doi.org/10.1007/BF02873097

Ren, J., Long, X.Y., Ji, J.F., Barrón, V., Torrent, J., Y. Wang, and S.Y. Xie (2020). Different enrichment patterns of pedogenic magnetic particles modulated by primary iron-phosphorous input, *Geophysical Research Letters.* https://doi.org/10.1002/essoar.10503638.1.

Schwertmann, U. (1964). Differenzierung der eisenoxide des bodens durch extraktion mit Ammoniumoxalat-Loesung, *Journal of Plant Nutrition and Soil Science*, *105* (3), 194-202. https://doi.org/10.1002/jpln.3591050303

Schwertmann, U. (1971). Transformation of Hematite to Goethite in Soils, *Nature*, *232*, 624-625. https://doi.org/10.1038/232624a0

Schwertmann, U. (1985). The effect of pedogenic environments on iron oxide minerals, *Advances in Soil Science*, *1*, 107-200. https://doi.org/10.1007/978-1-4612-5046-3_5

Tardy, Y., and D. Nahon (1985). Geochemistry of laterites, stability of Al-goethite, Al-hematite, and Fe^{3+}-kaolinite in bauxites and ferricretes; an approach to the mechanism of concretion formation, *American Journal of Science*, *285*(10), 865-903. https://doi.org/10.2475/ajs.285.10.865

Thompson, R., and F. Oldfield (1986). Environmental Magnetism. George Allen &Unwin, London. https://doi.org/10.1007/978-94-011-8036-8

Tong G.B., Zhang J.P., Yang X.D., Luo, B.X., Wang, Y.Z., and P.Y. Chen (1994). Late Cenozoic palynoflora and environmental changes in Yunnan-Guizhou Plateau, *Marine Geology and Quaternary Geology*, *3*, 91-104. https://doi.org/CNKI:SUN:HYDZ.0.1994-03-010

Torrent, J., V. Barrón, and Q. Liu (2006). Magnetic enhancement is linked to and precedes hematite formation in aerobic soil, *Geophysical Research Letters*, *33*, L02401. https://doi.org/10.1029/ 2005GL024818.

Torrent, J., Liu, Q.S., Bloemendal, J., and V. Barrón (2007). Magnetic enhancement and iron oxides in the upper Luochuan loess-paleosol sequence, Chinese loess Plateau, *Soil Science Society of America Journal*, *71*(5), 1570-1578. https://doi.org/ 10.2136/sssaj2006.0328

Trolard, F., and Y. Tardy (1987). The stabilities of gibbsite, boehmite, aluminous goethites and aluminous hematites in bauxites, ferricretes and laterites as a function of water activity, temperature and particle size, *Geochimica Et Cosmochimica Acta*, *51*(4), 945-957.

https://doi.org/10.1016/0016-7037(87)90 107-4

White, A.F., and A.E. Blum (1995). Effects of climate on chemical weathering in watersheds, *Geochimica et Cosmochimica Acta, 59*(9), 1729-1747. https://doi.org/10.1016/0016-7037(95)00078-E

Worm, H.U. (1998). On the superparamagnetic stable single domain transition for magnetite, and frequency dependence of susceptibility, *Geophysical Journal International*, *133*(1), 201-206. https://doi.org/10.1046/j.1365-246X.1998.1331468.x

Worm, H. U., and M. Jackson (1999). The superparamagnetism of Yucca Mountain Tuff, *Journal of Geophysical Research Solid Earth*, *104*(B11), 25415-25425. https://doi.org/10.1029/1999JB900285

Xie, Y.Y., Li, C.A.,Chang, X.Q. and J. Zhou (2003). Climatic evolution of loess on the northeastern margin of the Qinghai-Tibet Plateau and its coupling with plateau uplift, *Geology in China*, *30*(4), 436-441. https://doi.org/10.3969/j.issn.1000-3657.2003.04.019

Xie, L.S., Wu, P., Gu, S.Y., Liu, Q., Ge, J.J., and Z.X. Cao (2010). Erosion and accumulation records of red clay in the process of rocky desertification in karst mountainous area — Taking Mawoshan watershed in Wumeng Mountains as an example, *Soil and water Conversation in China*, *4*, 47-50. https://doi.org/10.3969/j.issn.1000-0941.2010.04.019

Xiong, S.F., Liu, T.S., and Z.L. Ding (2002). Paleoclimatic records of the loess in the vicinity of Beijing region during the last two Glacial-interglacial cycles and its implications, *Scientia Geographica Sinica, 1*, 18-23. https://doi.org/10.3969/j.issn.1000-0690.2002.01.004

Xu, Y.H. (1991). Southwest China Climate, 161pp, China Meteorological Press, Beijing.

Yang, X.L., Wang, P., and D.W. Gao (2019). Characteristics and lows of climate change in Wumeng mountain nature reserve from 1971 to 2015, *Journal of Northeast Forestry University*, *47*(9), 71-79. https://doi.org/10.13759/j.cnki.dlxb.2019.09.013

Yan, P., Yang, N., and B.Y. Ye (2011). The extraction and study of geomorphic surface in Guizhou and its adjacent areas based on ASTER-GDEM, *Remote sensing for land and resources*, *23*(2), 98-103. https://doi.org/10.3724/SP.J.1011.2011.00403

Yang, S.L., Fang, X.M., Li, J., An, Z.S., and F. Hitoshi (2001). Transformation functions of soil color and climate, *Science in China Series D Earth Science, 44*, 218–226. https://doi.org/10.1007/BF02911990

Yang, S.L., and Z.L. Ding (2003). Color reflectance of Chinese loess and its implications for climate gradient changes during the last two glacial-interglacial cycles, *Geophysical Research Letters*, *30*(20), 2058. https://doi .org/ 10.1029/2003 GL018346.